Journal of Magnetic Resonance 302 (2019) 21–27

Contents lists available at ScienceDirect

Journal of Magnetic Resonance

journal homepage: www.elsevier.com/locate/jmr

Chemically cross-linked polyacrylonitrile. A DMSO compatible NMR alignment medium for measurement of residual dipolar couplings and residual chemical shift anisotropies

Daiane S. Carvalho, Danilo G.B. da Silva, Fernando Hallwass, Armando Navarro-Vázquez *

Universidade Federal de Pernambuco, Departamento de Química Fundamental, CCEN, Recife, Pernambuco 50670-901, Brazil

ARTICLE INFO

Article history:
Received 26 January 2019
Revised 9 March 2019
Accepted 14 March 2019
Available online 15 March 2019

Keywords:
Alignment media
RDCs
RCSAs
Natural products
Structural elucidation
Stereochemistry

ABSTRACT

Chemically cross-linked polyacrylontrile polymer gels, have been prepared as an alignment medium compatible with DMSO-d_6. These gels allow measurement of residual dipolar couplings (RDCs) and residual chemical shift anisotropies (RCSAs) with good accuracy as tested with brucine and α-santonin natural compounds. The gels can be reversibly compressed allowing easy measurement of RCSAs. They also present good physical homogeneity, clean HSQC spectra with little background ^{1}H signals, and allow unambiguous referencing of ^{13}C spectra for RCSA extraction.

© 2019 Elsevier Inc. All rights reserved.

1. Introduction

NMR in weakly aligned media is nowadays a powerful tool in the structural elucidation of synthetic and natural organic compounds [1–3]. Alignment media allow the observation of residual anisotropic NMR parameters with residual dipolar coupling (RDCs) being the most prevalently employed. Anisotropic parameters provide structural information of non-local character that complements and extends conventional isotropic NMR mostly based on the use of Nuclear Overhauser effects (NOE) or the scalar coupling analysis (*J*), allowing the solution of otherwise intractable problems [4]. RDCs, for the most part one-bond proton carbon $^1D_{CH}$ couplings, have been used to solve conformation [5,6], relative configuration [4,7–10], and even constitution [11,12] of small organic molecules.

In addition to the RDCs, there has been recently considerable interest in the application of residual chemical shift anisotropy (RCSA) to structural problems. Similarly to RDCs, which report relative orientation of internuclear vectors, RCSAs report relative orientation of the chemical shielding tensors. Measurement of RCSAs is much more technically demanding since even minimal changes between the two degrees of alignment, needed to extract the anisotropic component of the chemical shift, cause important changes in the isotropic component. The first reported measurement of ^{13}C RCSAs for small molecules in weakly aligning media involved the use of variable angle probes [13]. Shortly after application to configurational analysis was described by Hallwass et al. [14] through the use of a rubber-based stretching device [15]. Other reported techniques for ^{13}C RCSA determinations made use of stretched gels in NMR tubes of two different inner diameter sections [16–18], compressible NMR gels [17,19] or lyotropic phases [20]. Simultaneous use of RDCs and RCSAs has been shown to be valuable for structural elucidation of challenging compounds [12,21]. A detailed protocol for the stretching/compressing gels technique has now been reported [22].

The use of mechanically compressible gels [23] is perhaps the simplest method to measure RDCs and RCSAs of small analytes. However until now only the $CDCl_3$ compatible PMMA gel has been used for simultaneous RDC/RCSA measurement [17,19]. It would be highly desirable to be able to employ the same methodology in DMSO-d_6 a NMR solvent very widely used in pharmaceutical research. Several weakly aligning media compatible with DMSO-d_6 have already been reported. Particularly interesting are lyotropic phases of grafted graphene oxide [24]. Several polymer gels have been also reported. Namely: stretched polyacrylonitrile (PAN) gels [25,26], cross-linked by application of β-radiation; acrylamide based ionic copolymers [27]; "universal" poly(ethylene oxide) gels

* Corresponding author at: Departamento de Química Fundamental, CCEN, Universidade Federal de Pernambuco, Av. Prof. Moraes Rego, 1235, Cidade Universitária, 50670-901 Recife, PE, Brazil.
E-mail address: armando.navarro@ufpe.br (A. Navarro-Vázquez).

https://doi.org/10.1016/j.jmr.2019.03.005
1090-7807/© 2019 Elsevier Inc. All rights reserved.

[28]; or the (2-hydroxyethyl methacrylate) (poly-HEMA) gels developed by Gil et al. [29]. Among all the DMSO compatible gels only poly-HEMA gels is known to be mechanically compressible in a reversible way. They present good homogeneity and allow extraction of RDCs in a single experiment due to the large difference in magnetic susceptibility between the free isotropic solvent and swollen polymer (~0.1 ppm). A caveat with many of these gels are the presence of strong residual signals in the HSQC spectrum, particularly from the protons in the mobile side-chain.

Aiming at the application of the mentioned compression technique to simultaneous RDC/RCSA measurement, in DMSO-d_6, we prepared here chemically crosslinked, and reversibly compressible, polyacrylonitrile gels as a new alignment system for organic compounds.

The polyacrylonitrile polymer is known to be insoluble in its own monomer as well as many organic solvents save for some polar solvents such as DMF or DMSO [30]. PAN gels were prepared by radical polymerization of acrylonitrile monomer in DMF using ethylene glycol diacrylate (EGDA) as a crosslinking agent in concentrations of 0.7 and 0.9% inside a 3 mm NMR tube. Best results were obtained at the concentration of 0.7 mol% of EGDA according to measured ^{2}H spectra (See SI). The gel was cut into 2.5 cm length pieces. The residual monomer was removed by washings with DMSO-d_6. After 10 h the gel swelled completely in DMSO. Experimental details are provided in the SI. Besides DMSO, the gels were found to swell also in DMF but not in chloroform, acetone or acetonitrile (See SI).

The performance of the new alignment medium for RDC/RCSA measurement was tested using brucine (**1**) and α-santonin (**2**) natural products (Fig. 1). The washed gels were swollen in a 5 mm NMR tube, followed by addition of a solution of 20 mg of the samples in 500 μL of DMSO-d_6. The gel was allowed to swell for 24 h before measurement in order to reach a good degree of physical homogeneity.

Spectra were measured at two different aligning conditions: the first one was the gel in the relaxed isotropic state and the second one the anisotropic compressed state. Compression was done using the commercial NewEra™ device [31]. Fig. 2 shows the ^{2}H DMSO-d_6 signal in these two alignment condition: (a) compressed and (b) relaxed gel. In the ^{2}H spectrum of the relaxed gel two signals are observed. The less intense peak corresponds to an isotropic layer of solvent surrounding the gel whereas the most intense one corresponds to the DMSO-d_6 inside the polymer [32]. When the gel is fully compressed, the DMSO-d_6 signal nicely splits in a 26.7 Hz doublet. Isotropic solvent is barely seen at this degree of compression. This observed splitting is much larger than the 3.8 Hz splitting reported for the poly-HEMA gels [29] for a crosslinking density of 0.2–0.3 mol%. The gels looked very homogeneous at bare sight and the FWHH linewidths were of 2.1 and 3.4 Hz for the gel in the relaxed and compressed state respectively (Fig. 2). For the sake of comparison linewidths of 1.5–3 Hz are typical of PMMA/poly-HEMA gels. When we used of a higher degree of cross-linking (0.9 mol%) gels were obtained which were too physically heterogeneous according to the observed ^{2}H lineshapes (See SI). We will show in the following section that the 0.7% cross-linking ratio presents an optimal degree of alignment for molecules of typical drug molecular sizes. One-bond ^{1}H–^{13}C couplings were measured using a *J*-scaled BIRD filtered experiment (*J*-scaling factor = 3) [33]. The correlation signals between carbon and hydrogen in the F1-coupled HSQC spectrum of C4-H4 and C1-H1 pairs are shown in (Fig. 3). RDCs values were obtained from the difference ($^1D_{CH}$ = $^1T_{CH} - {}^1J_{CH}$) (Fig. 3) between the $^1T_{CH}$ total coupling (compressed condition, green) and the $^1J_{CH}$ coupling (relaxed condition, red).

Fifteen RDC values, ranging from −33.6 to +34.1 Hz were measured as shown in Table 1. $^1D_{CH}$ value for methylene C15 could not be extracted due to the very low intensity of the signal in the anisotropic spectrum probably caused by excessive enlargement of the signal by the proton-proton couplings. As compared to poly-HEMA the present PAN gel presents a smaller difference in ^{1}H shifts between the isotropic layer and the gel (~0.03 ppm) which makes the gel unsuitable for one-shot experiments [29]. On the other hand, the lack of side-chain protons in acrylonitrile provides a clear background in HSQC experiments and only weak residual ^{1}H signals can be distinguished at ~3.1 and ~2.1 ppm. These signals, of very short T_2, can be further minimized using reverse linear prediction as shown in the SI.

The obtained RDCs were then applied to determine the relative configuration of brucine (**1**). From the possible 32 diasteroisomers only thirteen 3D geometries can be assembled by the Ligprep [34] program without excessive distortion [35]. Conformational spaces for these thirteen diastereoisomers were obtained using a molecular mechanics based conformational search (MMFF94) [36] in the Macromodel software [37]. A single conformer was found for all configurations in the chosen energy window after trivial MeO-rotamers were filtered out. The structures obtained were then reoptimized at the M062X/6-31+G** level of theory. Chemical shielding tensors were computed on the M062X structures at the PBE0/6-311+G** level (See SI for further details). All computations were done using the Gaussian09 software [38].

Experimental RDC values were then fitted for each of the thirteen diastereoisomers using the SVD procedure [39] as implemented in the MSpin-RDC program [40]. Quality of fit was

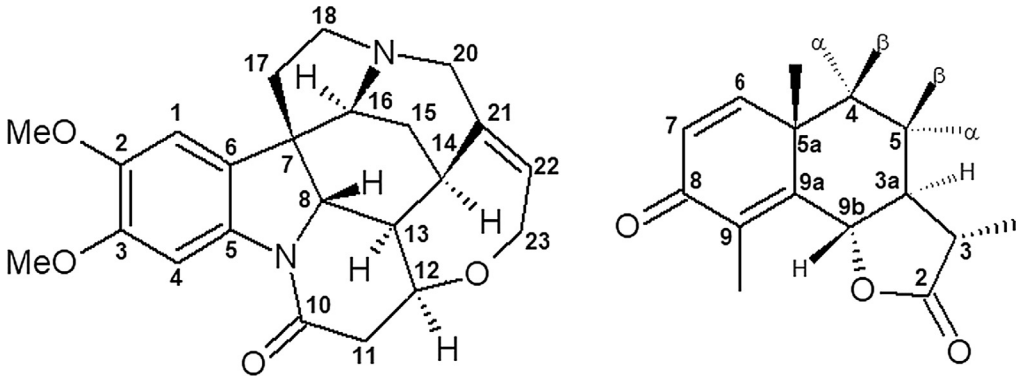

Brucine (1) **α-santonin (2)**

Fig. 1. Structures and numbering of brucine (**1**) and α-santonin (**2**).

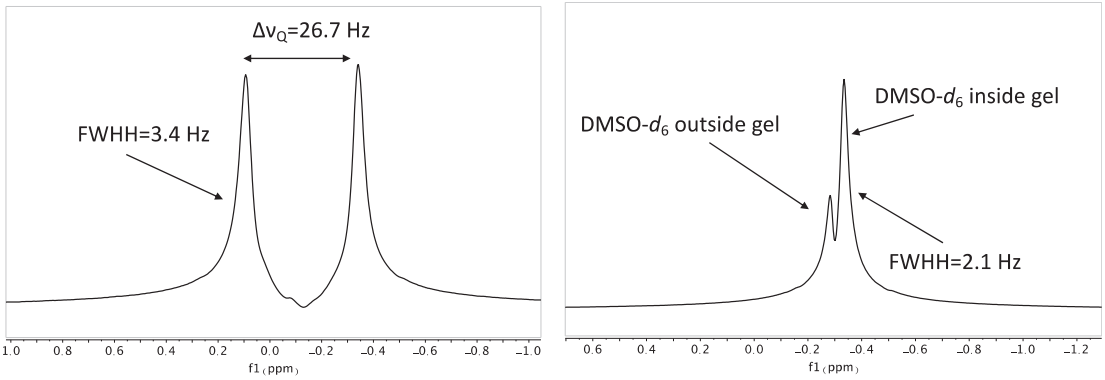

Fig. 2. ^{2}H NMR Spectra of PAN gel swollen in DMSO-d_6: (a) compressed and (b) relaxed alignment conditions.

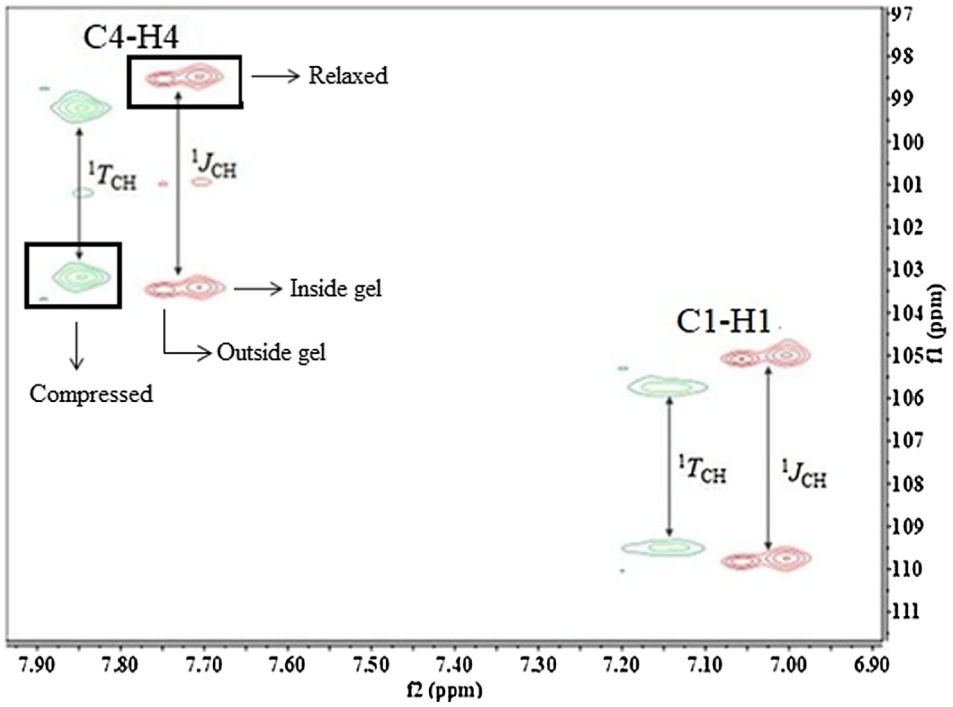

Fig. 3. Expansion of the superimposed ^{1}H-^{13}C coupled F1 HSQC NMR spectra showing C4-H4 and C1-H1 brucine (**T2**) signals at the compressed (green) and relaxed (red) conditions. (For interpretation of the references to colour in this figure legend, the reader is referred to the web version of this article.)

Table 1
Brucine scalar coupling constants $^{1}J_{CH}$, total splitting $^{1}T_{CH}$, and RDC values obtained experimentally in PAN gel/DMSO-d_6.

Atom	$^{1}J_{CH}$ (Hz)	$^{1}T_{CH}$ (Hz)	$^{1}D_{CH}$ (Hz)
1	159.3	125.6	−33.6
4	165.2	132.4	−32.7
8	145.3	166.7	21.3
11	130.2	133.3	3.0
12	150.4	162.9	12.4
13	126.1	131.8	5.7
14	132.4	144.2	11.8
16	147.0	181.1	34.1
17	133.0	138.8	5.0
18	138.4	149.7	11.2
20	138.5	131.3	−7.2
22	158.9	153.4	−5.0
23	141.2	162.3	21.0
MeO-C2[a]	144.2	151.5	7.2

[a] Signals partially overlapped.

expressed in terms of the Cornilescu *Q* factor [41]. A *Q* factor of 0.093 was obtained for the correct brucine configuration, while the second best structure scored a *Q* factor of 0.162. The measured RDCs providing therefore good discrimination between the structures. We excluded RDCs from the methoxy groups due to large overlapping of those signals and also for the sake of simplicity since MeO rotamers could then be safely discarded.

RCSAs values were obtained by simply comparing the chemical shift on the relaxed and compressed ^{13}C NMR spectra. A fundamental problem is how to reference the two spectra. A simple previously proposed solution is to employ a signal of the molecule with minimal chemical shielding tensor anisotropy [14]. The use of highly symmetric molecules, where RCSA vanishes, as TMS or CCl_4 has also been proposed [17,18]. However, here we observed that in going from the relaxed to the compressed state the ^{13}C polymer signals are barely distorted while the distance between the residual ^{13}C polymer signal and the DMSO-d_6 signal is kept constant. Therefore the use of the ^{13}C DMSO-d_6 solvent signals as

reference for RCSA measurement appeared to us as appropriate and simple and was the procedure employed here.

As reported, compression of the gel changes the polymer to solvent ratio as *a posteriori* correction is needed to account for the influence of solvation changes over the isotropic chemical shift [17]. We have previously shown that a scalar correction factor can be optimized simultaneously with alignment tensor parameters [19]. This factor is computed from the $\Delta\delta_{isotropic}$ chemical shift change between the signals in the relaxed gel and the isotropic solvent in the outer layer. Values of the experimentally measured RCSAs and $\Delta\delta_{isotropic}$ are shown in Table 2.

In Fig. 4 analysis and SVD fit of the RCSA data [40] provided a low *Q* factor (0.125) for the correct structure as well as good discrimination between stereoisomers with a *Q* = 0.216 for the second best structure. However, in this case the combination of RDCs and RCSAs did not improve the discrimination and *Q* factor increased to 0.196 while the second best score (*Q* = 0.217) barely changed. This was caused by the relatively large generalized angle β [42] (47°) between the RDC and RCSA derived alignment tensors [43]**.** The observed degree of order (GDO $\sim 1 \times 10^{-3}$) is similar to that reported for strychnine in a PMMA compressed gel [17] leading to *a priori* similar accuracy in the RDC/RCSA determination as reflected in the obtained quality factors not far from those reported.

Confirming the adequacy of the here synthesized gels RDCs and RCSA data were obtained and analyzed in the smaller α-santonin (**2**). RDCs from ∼−14 to +15 Hz were observed (See SI). Low quality factors were obtained when RDC and RCSA, either alone or in combination, were fit to all diastereoisomers of α-santonin **2** (Fig. 5). Excellent discrimination was observed in all the cases since the RDC/RCSA intertensor β angle was only 27°. Geometries and chemical shielding tensors were retrieved from the supporting information in the previous RDC/RCSA analysis of **2** in PMMA gels [19]. Additionally we also observed that the use of the more shielded signal as internal reference for measurement, as indicated in the published protocol [22], worsened the quality factor from 0.089 to 0.099 validating therefore the appropriateness of using the DMSO-d_6 ^{13}C signal as reference for this particular gel.

Very interestingly, examination of the alignment tensors showed that brucine does not align as expected for its molecular shape in a compressed gel, where a prolate inertia ellipsoid should prefer its shorter axis being parallel to the field rather than perpendicular. Unexpected orientations have been previously observed in particular occasions [17,44]. This behavior can be caused by the high polarity of the solvent that favor specific interaction between the polymer and the analyte (See figure in SI). Note however that a more conventional behavior was observed for α-santonin **2**. The RDC-derived tensor is rotated by 43° when compared to that reported previously using PMMA gels [19]. Differences in alignment behavior can be potentially exploited for multi-alignment media approaches [10]. The degree of order is similar to that reported for PMMA/$CHCl_3$ [19] albeit better quality factors and discrimination was observed here for the PAN/DMSO gel.

In summary, chemically cross-linked PAN is a very useful alignment medium for extraction of accurate RDCs and RCSAs in DMSO-d_6. When compared to other gels the gel can be easily prepared using common and cheap reagents, provides a good degree of alignment for compounds with typical drug molecular masses and very clean HSQC spectra due to the lack of protons in the monomer side chain.

2. Experimental section

2.1. Materials

The acrylonitrile monomer, (99%, Alfa Aesar, Tewksbury, USA) was purified prior to use by placing it in a small basic alumina column in order to remove the polymerization inhibitor. Ethylene glycol diacrylate (EGDA, 90%, Aldrich) was used as crosslinker. The AIBN (azobisisobutyronitrile) \ radical initiator was previously purified by recrystallization in MeOH. DMF (Dinâmica, Indaiatuba, São Paulo) was employed as received. Deuterated dimethylsulfoxide DMSO-d_6 (99.9% D atoms, CIL). α-santonin (**2**) (99%, Sigma Aldrich) and brucine (**1**) (99%, Dynamics) were used as test molecules.

2.2. Preparation of polyacrylonitrile gels (PAN)

A solution containing 500 μL (7.6 mmol) of acrylonitrile, 0.0015 g (8.86×10^{-3} mmol) of the azobisisobutyronitrile (AIBN) radical initiator, and 250 μL of dimethylformamide, was mixed with 9.5 μL (0.055 mmol) of ethylene glycol diacrylate (EGDA) crosslinker. The fraction of the EGDA crosslinking agent in the polymerization mixture was 0.7 mol%. The solution was transferred to a

Table 2
Brucine ^{13}C chemical shift, RCSA and $\Delta\delta_{isotropic}$ values obtained experimentally in PAN gel/DMSO-d_6.

Atom	δ (^{13}C) (ppm)	RCSA (ppb)	RCSA (Hz)	$\Delta\delta_{isotropic}$ (ppb)	$\Delta\delta_{isotropic}$ (Hz)
1	107.0	24.4	2.45	−79.4	−7.98
2	145.7	−17.7	−1.78	−82.3	−8.27
3	148.3	23.0	2.31	−42.4	−4.26
4	100.5	27.3	2.74	−61.5	−6.18
5	135.4	−58.6	−5.89	−61.5	−6.18
6	124.2	0.0	0.00	−195.8	−19.68
7	51.3	−9.7	−0.98	−36.1	−3.63
8	59.9	−27.7	−2.78	−98.9	−9.94
10	168.5	−28.1	−2.82	−27.5	−2.76
11	41.6	0.0	0.00	0.0	0.00
12	76.8	9.8	0.99	−58.6	−5.89
13	47.4	−12.0	−1.21	−83.3	−8.37
14	30.8	−13.6	−1.37	−97.1	−9.76
15	26.3	−13.6	−1.37	−120.1	−12.07
16	59.0	−13.4	−1.35	0.0	0.00
17	41.9	−10.8	−1.09	−126.8	−12.75
18	49.7	−15.9	−1.60	−53.5	−5.38
20	52.1	0.0	0.00	−122.4	−12.30
21	140.7	0.0	0.00	−350.2	−35.20
22	126.3	70.8	7.12	287.3	28.88
23	63.6	−28.1	−2.82	−51.9	−5.22
OMe-C2	56.0	−20.0	−2.01	−50.3	−5.06
OMe-C3	55.6	−33.7	−3.39	−33.0	−3.32

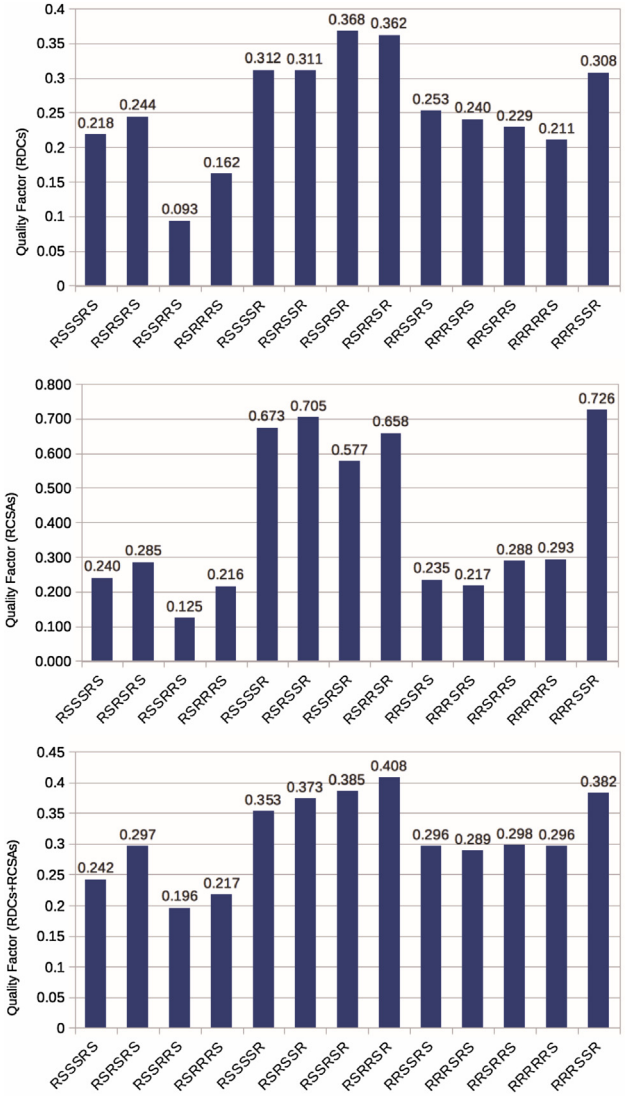

Fig. 4. *Q* factors for the thirteen generated configuration of brucine (**1**), applying three different procedure: using only RDCs data, using only RCSAs data, and combining RDCs and RCSAs data. *R*/*S* labels ordered after the 7, 8, 12, 13, 14, 16 stereocenters.

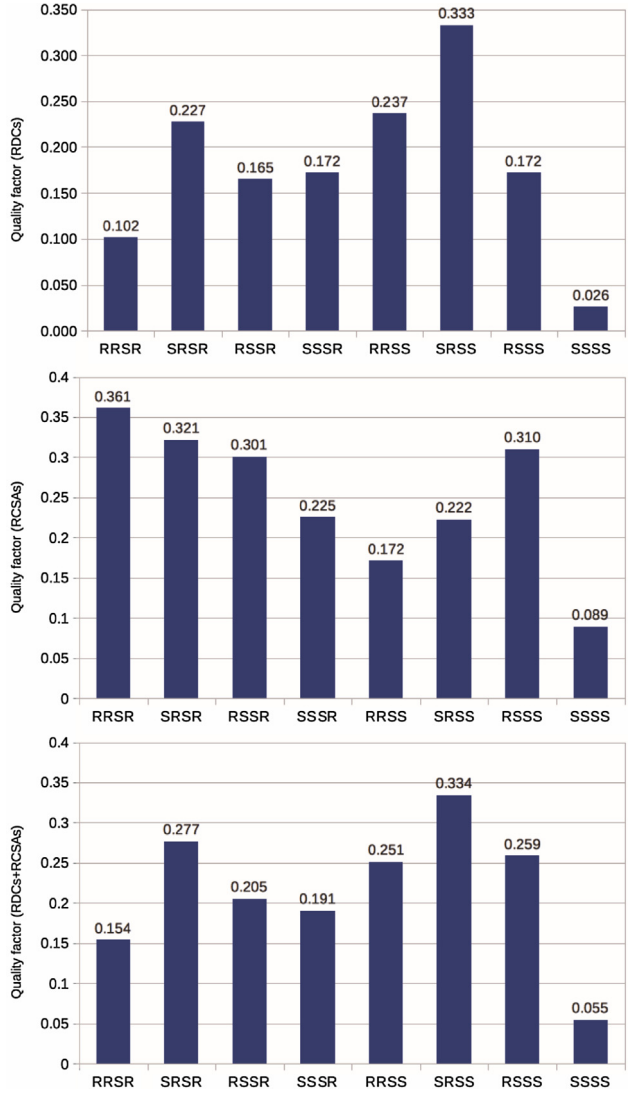

Fig. 5. *Q* factors for the eight possible relative configurations of α-santonin (**2**), applying three different procedure: using only RDCs data, only RCSAs data, and combining RDCs and RCSAs data. *R*/*S* labels ordered after the 3, 3a, 5a, 9b stereocenters (Fig. 1).

NMR tube (inner diameter = 3 mm), which was flame-sealed (purging of the tube with nitrogen or argon was not necessary). The NMR tube was then brought to the oven at 60 °C. Polymerization was performed for 24 h. After that the tube was taken from the oven. After breaking the upper part of the tubes the gels could be easily removed from them with the help of gentle circular movements. Gels were cut into 2.5 cm long stick. The dried gels were let to swell in DMSO-d_6 (1 ml) to remove DMF and unreacted monomer. The gel was let to wash for nearly 10–12 h in a small glass vial and the DMSO-d_6 (1 ml) was exchanged three more times. The vials should be closed since otherwise DMSO will capture humidity from the ambient and the water will cause shrinkage of the gel. After the last washing cycle the gel was let to dry at room temperature. The DMSO-d_6 was ^{1}H NMR spectra showed that acrylic monomer and initiator were successfully washed although in the case of α-santonin spectra some residual DMF could still be observed.

2.3. NMR experiments

All NMR experiments were performed on an Agilent 400 MHz spectrometer, operating at 298 K, with resonance frequencies of 399.75 MHz for ^{1}H, 61.36 MHz for ^{2}H, and 100.52 MHz for ^{13}C. The experiments were carried out using DMSO-d_6 (D, 99.9%) as solvent in a 5 mm NMR tube. ^{1}H, ^{13}C spectra were recorded using the s2pul sequence with broadband Waltz-16 ^{1}H decoupling [45], a total of 32k complex data points and acquisition time of 1.52 s. The spectra were and zero-filled to 128k complex points and baseline corrected using the Whitaker-Smoother algorithm [46] previous to RCSA measurement. F1-coupled HSQC spectra were acquired using a BIRD filtered *J*-scaled experiment [33] with a *J*-scale factor of 3 and 1024 and 4096 complex data points in the F2 and F1 dimensions respectively. RCSAs were measured by referencing to the DMSO-d_6 ^{13}C signal.

2.4. Alignment of brucine (*1*) and α-santonin (*2*) using PAN gel

The washed gel stick was inserted into a 5 mm NMR tube and swollen in a solution of 20 mg of brucine in 0.5 ml of DMSO-d_6. Compression of the gel was performed using the commercial compression apparatus designed by NewEra™ [31]. The alignment degree of the gels was verified by measuring the ^{2}H ν_Q quadrupolar splitting. An identical procedure was employed for α-santonin (**2**).

2.5. Molecular modeling

Diastereoisomers of brucine (**1**) were generated using Schrodinger Ligprep program [37]. A conformational search was performed at the MMFF94 [36] level using a short energy window of 6 kJ/mol. This resulted in one conformation per diastereoisomer after conformations corresponding to trivial methoxy group rotations were filtered out. Structures were refined at the M062X/6-31+G** level using the (99,159) *ultrafine* pruned grid. Implicit solvation was taken into account at the IEFPCM [47] level using Gaussian09 chloroform parameters. Chemical shielding tensors were computed on the M062X [48] geometries at the GIAO [49]/PBE0 [50]/6-311+G** level at the using DMSO parameters for IEFPCM solvation. Geometries (B3LYP/6-31G*) and chemical shielding tensors (PBE0/pcS-1 [51]) for all of the α-santonin (**2**) diastereoisomers were retrieved from previously published structures [19]. All computations were done using the Gaussian09 program [38].

2.6. RCSA and RDC analyses

RDCs and RCSAs were fitted to molecular structures using SVD [39] as implemented in the MSpin-RDC 2.4 program [40]. The scaling factor to take into account the contribution of changes in the isotropic part of the chemical shift was simultaneously optimized along alignment tensor components [19]. For the (3S,3aS,5aS,9bR) of α-santonin (**2**), which presented two conformations, the single tensor approximation was employed and the populations derived from the DFT energies through the Bolztamnn relationship at a temperature of 298.15 K. To combine RDCs and RCSAs the SVD fitting was performed expressing all experimental parameters in units of Hz [14].

Author contributions

The manuscript was written through contributions of all authors. All authors have given approval to the final version of the manuscript.

Acknowledgment

A.N-V and D.S.C. thank FACEPE for financial support APQ-0507-1.06/15) and a master studies fellowship (IBPG-0178-3.03/17). D.G. B.S thanks brazilian CAPES for a PhD fellowship. We also thank Dr. Ron Crouch for implementation of the *J*-scaled HSQC-F1 pulse sequence and Centro de Tecnologias Estratégicas do Nordeste (CETENE) for allocation of computer time.

Appendix A. Supplementary data

A PDF file with annotated 1D and 2D NMR spectra and molecular modelling as well as RDC and RCSA fitting details and photographs of swollen gels. A zip file containing MSpin-RDC inputs and outputs. Supplementary data to this article can be found online at https://doi.org/10.1016/j.jmr.2019.03.005.

References

[1] T. Claridge, High Resolution NMR techniques in Organic Chemistry, Elsevier, 2016.
[2] G.-W. Li, H. Liu, F. Qiu, X.-J. Wang, X.-X. Lei, Residual dipolar couplings in structure determination of natural products, Nat. Prod. Bioprospect. 8 (2018) 279–295, https://doi.org/10.1007/s13659-018-0174-x.
[3] V. Schmidts, Perspectives in the application of residual dipolar couplings in the structure elucidation of weakly aligned small molecules, Magn. Reson. Chem. 55 (2017) 54–60, https://doi.org/10.1002/mrc.4543.
[4] H. Sun, U.M. Reinscheid, E.L. Whitson, E.J. d'Auvergne, C.M. Ireland, A. Navarro-Vázquez, et al., Challenge of large-scale motion for residual dipolar coupling based analysis of configuration: the case of fibrosterol sulfate A, J. Am. Chem. Soc. 133 (2011) 14629–14636, https://doi.org/10.1021/ja205295q.
[5] C. Gayathri, M.C. de la Fuente, B. Luy, R.R. Gil, A. Navarro-Vázquez, Probing heterocycle conformation with residual dipolar couplings, Chem. Commun. 46 (2010) 5879–5881, https://doi.org/10.1039/C0CC01271H.
[6] C.S. Lancefield, A.M.Z. Slawin, N.J. Westwood, T. Lebl, The use of residual dipolar coupling for conformational analysis of structurally related natural products, Magn. Reson. Chem. 53 (2015) 467–475, https://doi.org/10.1002/mrc.4213.
[7] B. Böttcher, C.M. Thiele, Determining the stereochemistry of molecules from residual dipolar couplings (RDCs), eMagRes (2007), https://doi.org/10.1002/9780470034590.emrstm1194.
[8] E. Troche-Pesqueira, C. Anklin, R.R. Gil, A. Navarro-Vázquez, Computer-assisted 3D structure elucidation of natural products using residual dipolar couplings, Angew. Chem. Int. Ed. 56 (2017) 3660–3664, https://doi.org/10.1002/anie.201612454.
[9] G. Cornilescu, R.F. Ramos Alvarenga, T.P. Wyche, T.S. Bugni, R.R. Gil, C.C. Cornilescu, et al., Progressive stereo locking (PSL): a residual dipolar coupling based force field method for determining the relative configuration of natural products and other small molecules, ACS Chem. Biol. 12 (2017) 2157–2163, https://doi.org/10.1021/acschembio.7b00281.
[10] S. Immel, M. Köck, M. Reggelin, Configurational analysis by residual dipolar coupling driven floating chirality distance geometry calculations, Chem. Eur. J. 24 (2018) 13918–13930, https://doi.org/10.1002/chem.201802800.
[11] G. Kummerlöwe, B. Crone, M. Kretschmer, S.F. Kirsch, B. Luy, Residual dipolar couplings as a powerful tool for constitutional analysis: the unexpected formation of tricyclic compounds, Angew. Chem. Int. Ed. 50 (2011) 2643–2645, https://doi.org/10.1002/anie.201007305.
[12] Y. Liu, J. Saurí, E. Mevers, M.W. Peczuh, H. Hiemstra, J. Clardy, et al., Unequivocal determination of complex molecular structures using anisotropic NMR measurements, Science. 356 (2017) eaam5349, https://doi.org/10.1126/science.aam5349.
[13] G. Kummerlöwe, S.L. Grage, C.M. Thiele, I. Kuprov, A.S. Ulrich, B. Luy, Variable angle NMR spectroscopy and its application to the measurement of residual chemical shift anisotropy, J. Magn. Reson. 209 (2011) 19–30, https://doi.org/10.1016/j.jmr.2010.11.019.
[14] F. Hallwass, M. Schmidt, H. Sun, A. Mazur, G. Kummerlöwe, B. Luy, et al., Residual chemical shift anisotropy (RCSA): a tool for the analysis of the configuration of small molecules, Angew. Chem. Int. Ed. 50 (2011) 9487–9490, https://doi.org/10.1002/anie.201101784.
[15] P.W. Kuchel, B.E. Chapman, N. Müller, W.A. Bubb, D.J. Philp, A.M. Torres, Apparatus for rapid adjustment of the degree of alignment of NMR samples in aqueous media: Verification with residual quadrupolar splittings in 23Na and 133Cs spectra, J. Magn. Reson. 180 (2006) 256–265, https://doi.org/10.1016/j.jmr.2006.03.002.
[16] Y. Liu, J.H. Prestegard, A device for the measurement of residual chemical shift anisotropy and residual dipolar coupling in soluble and membrane-associated proteins, J. Biomol. NMR. 47 (2010) 249–258, https://doi.org/10.1007/s10858-010-9427-7.
[17] N. Nath, M. Schmidt, R.R. Gil, R.T. Williamson, G.E. Martin, A. Navarro-Vázquez, et al., Determination of relative configuration from residual chemical shift anisotropy, J. Am. Chem. Soc. 138 (2016) 9548–9556, https://doi.org/10.1021/jacs.6b04082.
[18] R.R. Gil, E. Hellemann, New stretching method for aligning gels. Its application to the measurement Residual Chemical Shift Anisotropies (RCSAs) without the need for isotropic shift correction, Chem. Eur. J. (2018), https://doi.org/10.1002/chem.201704541.
[19] F. Hallwass, R.R. Teles, E. Hellemann, C. Griesinger, R.R. Gil, A. Navarro-Vázquez, Measurement of residual chemical shift anisotropies in compressed polymethylmethacrylate gels. Automatic compensation of gel isotropic shift contribution, Magn. Reson. Chem. 19 (2018) 161, https://doi.org/10.1002/mrc.4711.
[20] Y. Liu, R.D. Cohen, K.R. Gustafson, G.E. Martin, R.T. Williamson, Enhanced measurement of residual chemical shift anisotropy for small molecule structure elucidation, Chem. Commun. 54 (2018) 4254–4257, https://doi.org/10.1039/C8CC00552D.
[21] E. Mevers, J. Saurí, Y. Liu, A. Moser, T.R. Ramadhar, M. Varlan, et al., Homodimericin A: a complex hexacyclic fungal metabolite, J. Am. Chem. Soc. 138 (2016) 12324–12327, https://doi.org/10.1021/jacs.6b07588.
[22] Y. Liu, A. Navarro-Vázquez, R.R. Gil, C. Griesinger, G.E. Martin, R.T. Williamson, Application of anisotropic NMR parameters to the confirmation of molecular structure, Nat. Protoc. 44 (2018) 1012, https://doi.org/10.1038/s41596-018-0091-9.
[23] C. Gayathri, N.V. Tsarevsky, R.R. Gil, Residual dipolar couplings (RDCs) analysis of small molecules made easy: fast and tuneable alignment by reversible compression/relaxation of reusable PMMA Gels, Chem. Eur. J. 16 (2010) 3622–3626, https://doi.org/10.1002/chem.200903378.
[24] W. Zong, G.-W. Li, J.-M. Cao, X. Lei, M.-L. Hu, H. Sun, et al., An alignment medium for measuring residual dipolar couplings in pure DMSO: liquid crystals from graphene oxide grafted with polymer brushes, Angew. Chem. Int. Ed. 55 (2016) 3690–3693, https://doi.org/10.1002/anie.201511435.
[25] G. Kummerlöwe, J. Auernheimer, A. Lendlein, B. Luy, Stretched poly (acrylonitrile) as a scalable alignment medium for DMSO, J. Am. Chem. Soc. 129 (2007) 6080–6081, https://doi.org/10.1021/ja071248s.
[26] G. Kummerlöwe, M. Behl, A. Lendlein, B. Luy, Artifact-free measurement of residual dipolar couplings in DMSO by the use of cross-linked perdeuterated

poly(acrylonitrile) as alignment medium, Chem. Commun. 46 (2010) 8273–8275, https://doi.org/10.1039/c0cc02730h.
[27] P. Haberz, J. Farjon, C. Griesinger, A DMSO-compatible orienting medium: towards the investigation of the stereochemistry of natural products, Angew. Chem. Int. Ed. 44 (2005) 427–429, https://doi.org/10.1002/anie.200461267.
[28] C. Merle, G. Kummerlöwe, J.C. Freudenberger, F. Halbach, W. Stöwer, C.L.V. Gostomski, et al., Crosslinked poly(ethylene oxide) as a versatile alignment medium for the measurement of residual anisotropic NMR parameters, Angew. Chem. Int. Ed. 52 (2013) 10309–10312, https://doi.org/10.1002/anie.201301929.
[29] L.F. Gil Silva, R. Santamaría-Fernández, A. Navarro-Vázquez, R.R. Gil, Collection of NMR scalar and residual dipolar couplings using a single experiment, Chem. Eur. J. 22 (2016) 472–476, https://doi.org/10.1002/chem.201503449.
[30] A. Charlesby, Atomic radiation and polymers, Elsevier (1960), https://doi.org/10.1016/C2013-0-07861-9.
[31] https://newera-spectro.com/compression-gel-device.
[32] E. Hellemann, R.R. Teles, F. Hallwass, W. Barros, A. Navarro-Vázquez, R.R. Gil, Mechanical behavior of polymer gels for RDCs and RCSAs collection: NMR imaging study of buckling phenomena, Chem. Eur. J. 22 (2016) 16632–16635, https://doi.org/10.1002/chem.201603333.
[33] C.M. Thiele, W. Bermel, Speeding up the measurement of one-bond scalar (1J) and residual dipolar couplings (1D) by using non-uniform sampling (NUS), J. Magn. Reson. 216 (2012) 134–143, https://doi.org/10.1016/j.jmr.2012.01.008.
[34] Ligprep. Schrödinger Release 2018-4: Maestro, Schrödinger, LLC, New York, 2018.
[35] G. Bifulco, R. Riccio, G.E. Martin, A.V. Buevich, R.T. Williamson, Quantum chemical calculations of 1J(CC) coupling constants for the stereochemical determination of organic compounds, Org. Lett. 15 (2013) 654–657, https://doi.org/10.1021/ol3034803.
[36] T.A. Halgren, Merck molecular force field. I. Basis, form, scope, parameterization, and performance of MMFF94, J. Comput. Chem. 17 (1996) 490–519, doi:10.1002/(SICI)1096-987X(199604)17:5/6<490::AID-JCC1>3.0.CO;2-P.
[37] Macromodel. Schrödinger Release 2018-4: Maestro, Schrödinger, LLC, New York, 2018.
[38] Gaussian 09, Revision B.01, M. J. Frisch, et al. Gaussian, Inc., Wallingford CT, 2016.
[39] J.A. Losonczi, M. Andrec, M.W. Fischer, J.H. Prestegard, Order matrix analysis of residual dipolar couplings using singular value decomposition, J. Magn. Reson. 138 (1999) 334–342, https://doi.org/10.1006/jmre.1999.1754.
[40] A. Navarro-Vázquez, MSpin-RDC. A program for the use of residual dipolar couplings for structure elucidation of small molecules, Magn. Reson. Chem. 50 (2012) S73–S79, https://doi.org/10.1002/mrc.3905.
[41] G. Cornilescu, A. Bax, Measurement of proton, nitrogen, and carbonyl chemical shielding anisotropies in a protein dissolved in a dilute liquid crystalline phase, J. Am. Chem. Soc. 122 (2000) 10143–10154, https://doi.org/10.1021/ja0016194.
[42] J. Sass, F. Cordier, A. Hoffmann, M. Rogowski, A. Cousin, J.G. Omichinski, et al., Purple membrane induced alignment of biological macromolecules in the magnetic field, J. Am. Chem. Soc. 121 (1999) 2047–2055, https://doi.org/10.1021/ja983887w.
[43] F. Kramer, M.V. Deshmukh, H. Kessler, S.J. Glaser, Residual dipolar coupling constants: an elementary derivation of key equations, Concepts Magn. Reson. Part A. 21A (2004) 10–21, https://doi.org/10.1002/cmr.a.20003.
[44] T. Niklas, C. Steinmetzger, F. Rüttger, D. Stalke, M. John, Distinct alignment of benzene derivatives in stretched polystyrene and polybutylacrylate gels: specific polymer-solute interactions, Magn. Reson. Chem. 55 (2017) 1084–1090, https://doi.org/10.1002/mrc.4633.
[45] A.J. Shaka, J. Keeler, T. Frenkiel, R. Freeman, An improved sequence for broadband decoupling: WALTZ-16, J. Magn. Reson. 52 (1983) 335–338, https://doi.org/10.1016/0022-2364(83)90207-X.
[46] J.C. Cobas, M.A. Bernstein, M. Martin-Pastor, P.G. Tahoces, A new general-purpose fully automatic baseline-correction procedure for 1D and 2D NMR data, J. Magn. Reson. 183 (2006) 145–151, https://doi.org/10.1016/j.jmr.2006.07.013.
[47] J. Tomasi, B. Mennucci, R. Cammi, Quantum mechanical continuum solvation models, Chem. Rev. 105 (2005) 2999–3093, https://doi.org/10.1021/cr9904009.
[48] Y. Zhao, D.G. Truhlar, The M06 suite of density functionals for main group thermochemistry, thermochemical kinetics, noncovalent interactions, excited states, and transition elements: two new functionals and systematic testing of four M06-class functionals and 12 other functionals, Theor. Chem. Account. 120 (2008) 215–241, https://doi.org/10.1007/s00214-007-0310-x.
[49] K. Wolinski, J.F. Hinton, P. Pulay, Efficient implementation of the gauge-independent atomic orbital method for NMR chemical shift calculations, J. Am. Chem. Soc. 112 (1990) 8251–8260, https://doi.org/10.1021/ja00179a005.
[50] C. Adamo, V. Barone, Toward chemical accuracy in the computation of NMR shieldings: the PBE0 model, Chem. Phys. Lett. 298 (1998) 113–119, https://doi.org/10.1016/S0009-2614(98)01201-9.
[51] F. Jensen, Basis set convergence of nuclear magnetic shielding constants calculated by density functional methods, J. Chem. Theory Comput. 4 (2008) 719–727, https://doi.org/10.1021/ct800013z.